TITLE:

SYNERGY-BASED SMALL-MOLECULE SCREEN USING A HUMAN LUNG EPITHELIAL CELL LINE YEILDS ΔF508-CFTR CORRECTORS THAT AUGMENT VX-809 MAXIMAL EFFICACY

AUTHORS & AFFILIATIONS:

Puay-Wah Phuan, Guido Veit, Joseph Tan, Ariel Roldan, Walter E. Finkbeiner,

Gergely Lukacs, and Alan S. Verkman

Departments of Medicine and Physiology (P.W.P, J.T, A.S.V.) and Department of Pathology (W.E.F.), University of California, San Francisco, California, 94143-0521, USA; Department of Physiology and Groupe de Recherche Axé sur la Structure des Protéine (GRASP) (G.V., A.R., G.L.) and Department of Biochemistry (G.L.), McGill University, Montreal, Quebec H3G 1Y6, Canada

RUNNING TITLE:

Synergy screen for ΔF508-CFTR correctors

CONTACT:

Corresponding author: Alan S. Verkman, 1246 Health Sciences East Tower, University of California,

San Francisco, CA 94143-0521, U.S.A.; Phone: 415-476-8530; Fax: 415-665 3847;

E-mail: Alan.Verkman@ucsf.edu; http: www.ucsf.edu/verklab

Number of text pages: 27

Number of figures: 7

Number of references: 45

Number of words in the *Abstract*: 249

Number of words in the *Introduction*: 630

Number of words in the *Discussion:* 906

Supplemental Tables: 3

Supplemental Figures: 5

Abbreviations: CFTR, cystic fibrosis transmembrane conductance regulator; ER, endoplasmic reticulum; CFBE, cystic fibrosis bronchial epithelial; MSD, membrane-spanning domains; NBD, nucleotide binding domains; YFP, yellow fluorescence protein; PBS, phosphate-buffered saline; DMSO, dimethyl sulfoxide; HRP, horseradish peroxidase; HA, human influenza hemagglutinin; VX-770, *N*-(2,4-di-*tert*-butyl-5-hydroxyphenyl)-4-oxo-1,4-dihydroquinoline-3-carboxamide; VX-809, 3-[6-[[[1-(2,2-difluoro-1,3-benzodioxol-5-yl)cyclopropyl]carbonyl]amino]-3-methyl-2-pyridinyl]-benzoic acid.

ABSTRACT

The most prevalent CFTR mutation causing cystic fibrosis, ΔF508, impairs folding of nucleotide binding domain 1 (NBD1) and stability of the interface between NBD1 and the membrane spanning domains (MSDs). The interfacial stability defect can be partially corrected by the investigational drug VX-809 or the R1070W mutation. 'Second-generation' ΔF508-CFTR correctors are needed to improve on the modest efficacy of existing CF correctors. We postulated that a second corrector targeting a distinct folding/interfacial defect might act in synergy with VX-809 or the R1070W suppressor mutation. A biochemical screen for ΔF508-CFTR cell surface expression was developed in a human lung epithelium- derived cell line (CFBE41o-) by expressing chimeric CFTRs with a horseradish peroxidase (HRP) in the fourth exofacial loop either in the presence or absence of R1070W. Using a luminescence read-out of HRP activity, screening of ~110,000 small molecules produced 9 novel corrector scaffolds that increased cell surface ΔF508-CFTR expression by up to 200 % in the presence vs. absence of maximal VX-809. Further screening of 1006 analogs of compounds identified from the primary screen produced 15 correctors with EC_{50} <5 µM. 8 chemical scaffolds showed synergy with VX-809 in restoring chloride permeability in ΔF508-expressing A549 cells. An aminothiazole increased chloride conductance in human bronchial epithelial cells from a ΔF508 homozygous subject beyond that of maximal VX-809. Mechanistic studies suggested that NBD2 is required for the aminothiazole rescue. Our results provide proof-of-concept for synergy screening to identify second-generation correctors, which, when used in combination, may overcome the 'therapeutic ceiling' of first-generation correctors.

MOL #92478

INTRODUCTION

CFTR (cystic fibrosis transmembrane conductance regulator) is a cAMP-regulated chloride channel expressed in airway and other epithelia. CFTR is a large membrane glycoprotein containing two membrane-spanning domains (MSD1-2) and three cytoplasmic domains, which include two nucleotide binding domains (NBD1-2) and a regulatory domain (Riordan, 2005). Mutations in CFTR cause the genetic disease cystic fibrosis (CF) in which lung infection and mucus accumulation can lead to life-threatening deterioration of lung function. The most common CFTR mutation, deletion of phenylalanine at residue 508 (ΔF508), is present in at least one allele in ~ 90% of CF patients. The ΔF508 mutation produces CFTR misfolding, with retention at the endoplasmic reticulum (ER), accelerated CFTR degradation at the ER and periphery, and impaired chloride channel gating (Balch et al.; 2011, Du et al., 2009; Gadsby et al., 2006; Riordan, 2008). The reduced plasma membrane chloride permeability in CFTR-expressing cells containing the ΔF508 mutation has been proposed to produce the clinical phenotype by a variety of mechanisms involving abnormal airway surface liquid homeostasis, reduced gland fluid secretion, defective immune cell function, and others (Boucher et al., 2004; Cohen and Prince, 2012; Zielenski et al., 2000).

There has been considerable effort and progress in the development of CFTR-targeted small-molecule therapeutics for CF (Ashlock and Olson, 2011). The CFTR 'potentiator' VX-770 (Ivacaftor), which corrects defective channel gating of some CFTR mutants, has been approved for CF therapy caused by the defective channel gating but unimpaired cellular processing and plasma membrane targeting of the G551D-CFTR mutation (Accurso et al., 2010; Van Goor et al., 2009). Several small-molecule 'correctors' of ΔF508-CFTR cellular processing have been identified (Pedemonte et al., 2005a, 2005b; Phuan et al., 2011; Robert et al., 2010; Van Goor et al., 2006; Yu et al., 2008). VX-809 is in clinical trials for CF caused by the ΔF508 mutation (Clancy et al., 2012). However, to date VX-809 and other correctors show limited efficacy in primary human bronchial cell cultures from ΔF508-homozygous CF patients, restoring only ~15 % of full CFTR activity found in cultures from non-CF patients (Van Goor et al., 2011). Clinical trials with VX-809, alone or together with VX-770, have thus far shown minimal efficacy (NCT01225211). The need for 'second-generation' correctors with

improved efficacy has been widely acknowledged (Hanrahan et al., 2013; Lukacs and Verkman, 2012; Okiyoneda and Lukacs, 2012).

Here, we report proof-of-concept for a 'synergy screening' approach to identify second-generation ΔF508-CFTR correctors. The idea for synergy screening is that global misfolding and dysfunction of ΔF508-CFTR can be efficiently reversed by stabilizing two major structural deficiencies; the NBD1 stability and the NBD-MSDs interfacial defects (Rabeh et al., 2010), which is supported by data from suppressor mutations and corrector combinations (Okiyoneda et al., 2013). While VX-809 is unable to restore the thermal stability of the isolated ΔF508-NBD1 (Farinha et al., 2013; Okiyoneda et al. 2013; Ren et al., 2013), it is thought to directly stabilize the interface between NBD1 and MSDs (Farinha et al., 2013; Okiyoneda et al. 2013; Ren et al., 2013; Van Goor et al. 2011). Combining genetic modification (e.g. suppressor mutation in the NBD1; 3S) of the ΔF508-NBD1 or chemical chaperones with VX-809 produced robust potentiation of VX-809 effect on the folding and cell surface expression of ΔF508-CFTR (Okiyoneda et al., 2013). Therefore, novel corrector molecules targeting either the NBD1 and/or its interface defects should be preferentially identified by screening in the background of VX-809 or \the interface-stabilizing mutation R1070W. To this end, here we established, using human lung epithelium-derived cell lines (CFBE41o-, Ehrhardt et al., 2006; Veit et al., 2012), a novel biochemical screening procedure. Compounds were identified that, when combined with VX-809, increased correction efficacy beyond that of maximal VX-809 alone, supporting the idea of synergy screening and corrector combination therapy for CF caused by the ΔF508 mutation.

MATERIALS AND METHODS

Cell lines

Doxycycline-inducible expression systems were generated by lentivirus transduction using the Lenti-X TetON Advanced Inducible Expression System (Clontech, Mountain View, CA) as described (Veit et al, 2012). For expression of extracellular HRP-tagged CD4TM- ΔF508-NBD1-1S chimeras the extracellular CD4 domain of the previously described CD4T-ΔF508-NBD1-1S (Rabeh et al., 2012) was replaced in-frame with the catalytic domain of horseradish peroxidase (HRP). Madin-Darby canine

kidney (MDCK) type II cells stably expressing HRP-CD4TM-ΔF508-NBD1-1S were maintained in Dulbecco's modified Eagle's medium (DMEM) (Invitrogen, Carlsbad, CA) supplemented with 10% fetal bovine serum (FBS) under puromycin (3 μg/ml) and G418 selection (0.2 mg/ml). BHK cells expressing ΔF508 and ΔF508-1218X CFTR-3HA variants have been described (Okiyoneda et al., 2013). The cloning and characterization of 3HA-tagged variants of ΔF508-CFTR, R1070W-ΔF508-CFTR, and 3S-ΔF508-CFTR- (containing the F494N, Q637R and F429S NBD1 suppressor mutations) have been described (Okiyoneda et al., 2013). To replace the 3HA tag in the ΔF508-CFTR variants, the horseradish peroxidise isoenzyme C was introduced into the 4th extracellular loop by using the EcoRV/AvrII restriction sites with a 5' linker (ctcgaatcaggaggtagtggtggcggaagt) linker, but without a 3' linker. CFBE41o- cells were grown in minimal essential medium (MEM, Invitrogen) supplemented with 10% FBS, 2 mM L-glutamine and 10 mM HEPES. For propagation, the CFBE41o- cells were cultured in plastic flasks coated with an extracellular matrix consisting of 10 μg/ml human fibronectin, 30 μg/ml collagen from calf skin (Sigma-Aldirch) and 100 μg/ml bovine serum albumin (Sigma-Aldrich) diluted in LHC-8 basal medium (Invitrogen).

For high-throughput screening, CFBE41o- Tet-on cells were plated in black, 96-well microplates (Costar, Corning Inc.) at 15,000 cells/well. ΔF508-CFTR expression was induced 24 h after plating with 0.5 μg/ml doxycycline treatment for 2 d before screening. A549 lung epithelial cells (ATCC CCL-185) stably expressing ΔF508-CFTR (Pedemonte et al., 2010) were provided by Dr. Luis Galietta (Genoa, Italy) and cotransfected with halide-sensitive green fluorescent protein YFP-H148Q/I152L/F46L (Galietta et al, 2001). A549 cells were cultured in DMEM/Ham's F12 (1:1) containing 10% FBS, 2 mM L-glutamine, 100 U/ml penicillin and 100 μg/ml streptomycin. For functional assay, A549 cells were plated in black, 96-well microplates (Costar, Corning Inc.) at 10,000 cells/well. For short-circuit current measurements, primary cultures of human CF bronchial epithelial cells were isolated and grown at an air-liquid interface for at least 21 days on cell culture inserts (Snapwell; Corning, Lowell, MA) and used when transepithelial resistance was > 1000 $\mu\Omega/cm^2$, as described (Yamaya et al., 1992; Fulcher and Randell, 2013).

Compounds

A total of 110,000 diverse drug-like synthetic compounds (>90% with molecular size 250-500 Da; ChemDiv Inc.) were used for screening. For optimization, 1006 commercially available analogs from different classes of active compounds from the primary screens were tested.

Screening procedures

Screening was carried out using a Beckman Coulter (Fullerton, CA) platform (Biomek FX). In one set of assays R1070W-ΔF508-CFTR-HRP (R1070W-HRP) expressing CFBE41o- cells were incubated with 100 μL medium containing 25 μM test compounds and 0.5 μg/ml doxycycline, for 24 h at 37 °C. In a second set of assays ΔF508-CFTR-HRP (ΔF508-HRP) expressing CFBE41o- cells were incubated with 100 μL medium containing 25 μM test compounds, 2 μM VX-809 and 0.5 μg/ml doxycycline for 24 h at 37 °C. All compound plates contained negative controls (DMSO vehicle) and positive controls (2 μM VX-809). In both assays the cells were washed 4 times with PBS, and HRP activity was assayed by addition of 50 μL/well of HRP-substrate (WesternBright Sirius Kit, Advansta Corp, Menlo Park, CA). After shaking for 5 min, chemiluminescence was measured using a TECAN Infinite M1000 plate reader (TECAN Groups Ltd, Mannedorf, Switzerland) equipped with automated stacker (integration time, 100 ms). Z' is define as = 1-[(3 x standard deviation of maximum signal control + 3 x standard deviation of minimum signal control) / absolute(mean of maximum signal control-mean of minimum signal control)] (Zhang et al., 1999).

Functional assays

A549 cells expressing ΔF508-CFTR-YFP were grown at 37 °C / 5% CO_2 for 18-24 h after plating. The cells were then incubated with 100 μL of medium containing test compounds for 18-24 h. At the time of the assay, cells were washed with PBS and then incubated for 10 min with PBS containing forskolin (20 μM) and genistein (50 μM). Each well was assayed individually for I⁻ influx by recording fluorescence continuously (200 ms per point) for 2 s (baseline) and then for 12 s after rapid addition of 165 μL PBS in which 137 mM Cl⁻ was replaced by I⁻. Initial I⁻ influx rate was computed by fitting the final 11.5 seconds

7

of the data to an exponential for extrapolation of initial slope, which was normalized for background-subtracted initial fluorescence. All compound plates contained negative controls (DMSO vehicle) and positive controls (5 μM VX-809). Fluorescence was measured using a TECAN Infinite M1000 plate reader equipped with a dual syringe pump (excitation/emission 500/535 nm).

Short-circuit current measurements

Test compounds (without or with 10 μM VX-809) were incubated with primary human CF bronchial epithelial cells from ΔF508-CFTR–homozygous subjects at the basolateral side for 18-24 h at 37 °C prior to measurements. The apical and basolateral chambers contained identical solutions: 130 mM NaCl, 0.38 mM KH_2PO_4, 2.1 mM K_2HPO_4, 1 mM $MgCl_2$, 1 mM $CaCl_2$, 25 mM $NaHCO_3$ and 10 mM glucose. Solutions were bubbled with 5% CO_2/95% O_2 and maintained at 37 °C. Hemichambers were connected to a DVC-1000 voltage clamp (World Precision Instruments Inc., Sarasota, FL) via Ag/AgCl electrodes and 1 M KCl agar bridges for recording of short-circuit current.

CFTR plasma-membrane (PM) density measurements

The PM density of 3HA-tagged CFTR variants was determined by cell surface ELISA (Okiyoneda et al., 2010). HRP-tagged CFTR PM density was measured in a VICTOR Light plate reader (PerkinElmer, Waltham, MA) after addition of 50 μl/well HRP-Substrate (SuperSignal West Pico, Thermo Fisher Scientific, Waltham, MA). PM density measurements were normalized with cell viability determined by Alamar Blue assay (Invitrogen, Carlsbad, CA).

Differential scanning fluorimetry (DSF)

Isolation of recombinant human NBD1 containing a single suppressor mutation (1S; F494N) and melting temperature measurement were performed as described (Rabeh et al., 2012). DSF scans of NBD1 (6 μM) were done in 150 mM NaCl, 20 mM $MgCl_2$, 10 mM HEPES and 2.5 mM ATP, pH 7.5 using a Stratagene Mx3005p (Agilent Technologies, La Jolla, CA) qPCR instrument in the presence of 2× Sypro Orange. These studies were performed on recombinant NBD-1S, since we have not seen discernible

differences in the relative thermal stability NBD1 and NBD-1S in the presence of the corrector panel

(Rabeh et al., 2012).

RESULTS

Development and validation of synergy-based CFTR screens

Primary screening was done using two stably transfected human lung epithelium-derived (CFBE41o-) cell lines (Ehrhardt et al., 2006). One screen ('ΔF508 screen') (Fig. 1A) utilized CFBE41o- cells transfected with human ΔF508-CFTR with a horseradish peroxidase (HRP) inserted in its fourth extracellular loop (ΔF508-HRP CFBE41o-). A second screen ('R1070W screen') (Fig. 1B) utilized CFBE41o- cells transfected with ΔF508-CFTR-HRP containing a R1070W mutation (R1070W-HRP CFBE41o-). Cells were cultured on 96-well plates and CFTR synthesis was induced 48 h prior to screening. Cells were grown to confluence prior to addition of test compounds. For the ΔF508 screen cells were incubated with test compounds (at 25 µM) together with 2 µM VX-809; for the R1070W screen cells were incubated with test compounds (at 25 µM) alone. The 25 µM concentration was chosen following initial small-scale screens showing a small percentage of active compounds. After incubation for 18-24 h at 37 ℃, cells were washed and HRP substrate was added for luminescence read-out. Test compounds that were cytotoxic at the screening concentration (25 µM) will result in reduced luminescence signal.

VX-809 produced a concentration-dependent increase in HRP luminescence signal after incubation with cells at 37 ℃ or 27 ℃ (Fig. 1A and 1B) in both cell lines, with similar EC_{50} of ~0.3 µM. In ΔF508-HRP CFBE41o- cells at 37 ℃ VX-809 increased signal maximally to ~250 luminescence arbitrary units (a.u.) over DMSO-control baseline of ~60 a.u., representing a ~4-fold signal increase. Similarly, with the R1070W-HRP CFBE41o- cells, VX-809 increased signal maximally to ~220 a.u. over DMSO-control baseline of ~85 a.u., representing a ~2.5-fold signal increase (bar graphs in Fig. 1A and 1B). Therefore, both cell lines produced robust signals with a good dynamic range for high-throughput screening.

Low-temperature rescue (27 ℃) of ΔF508-CFTR increased HRP luminescence signal by ~2-fold (compared with 37 ℃) in ΔF508-HRP CFBE41o- cells and ~3-fold in R1070W-HRP CFBE41o- cells. VX-809 and low-temperature together further increased HRP luminescence. EC_{50} values were 30 nM and 78 nM in the low-temperature rescued ΔF508-HRP and R1070W-HRP CFBE41o- cells,

10

respectively.

Preferential correction of ΔF508-CFTR-3HA with the NBD1 stabilizing 3S mutations (F494N,

Q637R and F429S) compared to CFTR carrying the R1070W interface stabilizing mutation has been

taken as evidence that VX-809 preferentially stabilizes the interface between NBD1 and MSDs but not

the NBD1 folding defect CFTR (Okiyoneda et al., 2013). This was preserved in the CFTR-HRP context,

indicating that the HRP fusion preserved behavior of the ΔF508 variants (Supplemental Fig. 1). The

relative insensitivity of R1070W-HRP to VX-809 was utilized to identify correctors that act in synergy

with VX-809.

Identification of ΔF508-CFTR correctors by synergy screens

A total of 110,240 drug-like small synthetic molecules were tested in the ΔF508 and R1070W

screens. As summarized in Fig. 2A, in the ΔF508 screen 164 active compounds were identified based

on >50% increase in luminescence signal over that of 2 μM VX-809 alone. After re-testing, five

compounds, grouped into three classes, were confirmed from the ΔF508 screen. Fig. 2B shows the

structures of the three most active compounds, H-01, J-01 and K-01. For the R1070W screen 25 active

compounds were identified based on >50% increase in luminescence signal over that of DMSO. After

retesting, nine compounds, grouped into six classes, were confirmed from the R1070W screen. Fig. 2D

shows structures of the six most active compounds, A-01, B-01, C-01, D-01, E-01 and F-01.

Because different small molecule collections were used for the ΔF508 and R1070W screens, we

cross-tested all active correctors in both the ΔF508-HRP and R1070W-HRP CFBE41o- cell lines

(Supplemental Fig. 2). Five compounds, A-01, B-01, C-01, H-01 and K-01, were active in both cell lines.

However, compounds D-01, E-01 and F-01, discovered from the R1070W screen, were not active in

ΔF508-HRP CFBE41o- cells. J-01, discovered from the ΔF508 screen, was not active in R1070W-HRP

CFBE41o- cells. We further tested the concentration-dependent activities of A-01, B-01, H-01 and K-01

(in the presence of 2 μM VX-809) in ΔF508-HRP CFBE41o- cells (Fig. 3A). H-01 was the most potent

corrector with EC_{50} ~1.5 μM and maximal signal >300% over that produced by 2 μM VX-809. However,

H-01, when tested alone in ΔF508-HRP CFBE41o- cells, had little activity (Supplemental Table 1). We

also measured the concentration-dependent activities of A-01, B-01, D-01, H-01 and K-01 (Fig. 3B) in

R1070W-CFBE41o- cells and found that D-01 is the most potent corrector with EC_{50} ~1.2 μM and

maximal signal ~65% of that produced by 2 μM VX-809. Supplemental Table 1 and Supplemental Fig. 2

summarize EC_{50} of all compounds in both cell lines, with and without 2 μM VX-809. We conclude that

H-01 and D-01 are the most active class of compounds discovered from the screens.

To confirm that the HRP luminescence assay reports the apical plasma membrane CFTR in the

CFBE41o- cells, the relative correction determined in the HRP assay was compared to that detected

using a extracellular 3xHA tagged ΔF508-CFTR (ΔF508-CFTR-3HA) expressed in CFBE41o- cells by

cell-surface ELISA, as described (Veit et al., 2012). A linear correlation was found for a panel of

correctors (Fig. 3C), confirming the results obtained from the CFTR-HRP luminescence assay.

Structure-activity analysis

1006 commercially available analogs of active compounds were tested to establish

structure-activity relationships. Fig. 4A shows concentration-dependence data of H analogs (in the

presence of 2 μM VX-809) in ΔF508-HRP CFBE41o- cells. Several class H analogs increased HRP

luminescence with low micromolar EC_{50}. Similar compound potency and efficacy was found for class D

analogs in R1070W-HRP CFBE41o- cells (Fig. 4C). Supplemental Table 2 and Supplemental Fig. 3

summarize EC_{50} for the most active class D and H analogs. We found that the most active analogs have

similar activities as the original compounds identified in the primary screen. Structural determinants of

activity for class D and H compounds are summarized in Figs. 4B and 4D. Class D correctors are

2-aminothiazoles, with best activities found for analogs with R^1 substituents phenyl, thiophene and furan.

Electron-withdrawing aromatic groups at the R^1 position, such as nitrophenyl, biphenyl, pyridine and

naphthalene, reduced activity. Active groups on the thiazole include methyl (for example, D-02, D-03),

naphthalenes (D-04, D-05) and 6-methyl-cyclohexyl (D-01) rings. Rings such as hindered

t-butyl-cyclohexyl and cyclohexanone reduced activity. Class H analogs contained a unique

dihydrospiro-indene scaffold. Analogs with different substituents on the phenyl ring (R^1) and on the

nitrogen (R^2) were examined. For R^1, class H analogs with the phenyl ring substituted at the 4-position

with halides and electron-neutral alkyl groups were active. Substitution at the 2-position on the phenyl ring reduced activity. For the R^2 position, analogs with naphthalene and di-substituted phenyl rings had greatest activity, whereas electron-withdrawing group such as benzyl, nitro-substituted phenyl and cyclohexyl rings reduced activity.

Functional measurements of halide transport in human A549 lung epithelial cells

A cell-based fluorescence assay of iodide influx was used for functional studies. Human lung epithelium-derived A549 cells stably expressing ΔF508-CFTR and an iodide-sensitive YFP were incubated with the test compounds, without or with VX-809, at 37 °C for 24 h (Fig. 5A). Iodide influx was measured by addition of extracellular iodide in the presence of maximal concentration of a potentiator (50 μM genistein) and a cAMP agonist (20 μM forskolin). Representative iodide influx data for fluorescence plate reader assays of D-01 and H-01, alone or with 2 μM VX-809, are shown in Fig. 5B. Increased ΔF508-CFTR conductance is seen as a greater negative slope. Concentration-dependence data for A-01, B-01, D-01, H-01, K-01, without and with VX-809, are shown in Fig. 5C. Supplementary Table 3 summarizes EC_{50} and V_{max} values. The compounds showed moderate functional activity in A549 cells. For example, the EC_{50} of aminothiazole D-01 is 2.9 μM with V_{max} 43% of that produced by 2 μM VX-809. When added together with VX-809, most correctors increased ΔF508-CFTR function by ~20% over maximal VX-809 (2 μM). D-01 and H-01 were most active, with similar EC_{50} ~0.6 μM and V_{max} ~120%.

Mechanistic studies of corrector action

To assess whether the correctors identified here can restore ΔF508-NBD1 stability in vivo, cell surface expression of the HRP-CD4-ΔF508-NBD1-1S chimera was measured in MDCK-II cells. This approach probes the *in vivo* conformational stability of the isolated NBD1 tethered to a reporter molecule, as based on our observation that the CD4-ΔF508-NBD1 chimera cell surface density is proportional to NBD1 thermal stability (Rabeh et al., 2012). The plasma membrane density of the HRP-CD4-ΔF508-NBD1-1S chimera was increased in the presence of 30 μM C-01 to the level detected

13

in the presence of the chemical chaperone glycerol (5%) (Fig. 6A) (Sato et al., 1996). The C-01 induced in vivo rescue could be accounted for by the direct thermo-stabilization of the NBD1-1S, based on the melting temperature (T_m) shift of the domain as monitored by differential scanning fluorimetry (Rabeh et al., 2012). 30 µM C-01 was able to increase the NBD1-1S T_m to that found in the presence of 5% glycerol (Fig. 6B and data not shown). C-01 is one of few compounds so far described to act directly on NBD1 (Okiyoneda et al., 2013). Even though this compound acted only at 30 µM and showed limited efficacy on full-length CFTR, its scaffold might be used for future SAR studies.

It has been demonstrated that corrector 4 (C4)-mediated rescue of the ΔF508 CFTR folding defect requires the presence of the NBD2 in CFTR (Okiyoneda et al., 2013). To investigate whether any of the correctors identified here may target the NBD2 interface, their synergy with C4 was evaluated in R1070W-HRP CFBE41o- cells using the HRP luminescence assay. While the relative rescue efficiency of A-01, B-01, C-01 and K-01 did not change in the presence of C4, the D-01 rescue effect was prevented by C4 (Fig. 6C). This observation suggests that D-01 and C4 may target an overlapping site on NBD2. In agreement, truncated ΔF508-CFTR-3HA lacking the NBD2 (ΔF508-1218X-CFTR) prevented rescue by D-01 regardless of the presence of VX-809 (Fig. 6D), supporting the conclusion that NBD2 may represent one of the targets of D-01. These results provide a mechanistic basis of the synergistic action of D-01 with VX-809 as seen in the functional measurements.

Short-circuit measurements in primary cultures of ΔF508-homozygous human bronchial CF epithelial cells

Functional assays were also done in well-differentiated primary cultures of human bronchial epithelial cells from a ΔF508-CFTR–homozygous subject. Short-circuit current was measured across electrically tight polarized monolayers cultured on porous supports at an air-liquid interface in which test compounds were added to the bath solution for 18-24 h prior to measurements. Sodium current was blocked with amiloride. Cells incubated with 10 µM VX-809 alone (Blanchard et al., 2014) showed increased short-circuit current in response to forskolin and genistein, which was inhibited by CFTR$_{inh}$-172 (Fig. 7A). Little current was seen in the absence of VX-809. D-01 at 30 µM together with

14

10 µM VX-809 increased chloride conductance more than that of VX-809 alone. D-01 alone did not

increase current in the bronchial epithelial cells. The other correctors, including H-01, when tested in

human bronchial epithelial cells of the same ΔF508-CFTR–homozygous subject, showed small increases

in chloride current (Supplemental Fig. 4). Fig. 7B summarizes chloride current responses following

forskolin and forskolin + genistein. Chloride current increased by 2.3 µA/cm^2 (forskolin) and 3.4

µA/cm^2 (forskolin + genistein) when cells were treated with D-01 and VX-809 versus VX-809 alone.

The fractional stimulation of short-circuit current by forskolin alone compared to the maximum current

measured in the presence of forskolin and genistein was increased two-fold by D-01, suggesting that the

corrector combination favors the ΔF508-CFTR native-like conformation, which is more susceptible to

activation by forskolin and less dependent on genistein.

DISCUSSION

This study was done to investigate the idea that a synergy screen might identify ΔF508-CFTR correctors, which, when used in combination, would have greater maximal efficacy than individually used correctors. The underlying hypothesis is that distinct structural defects in ΔF508-CFTR each require correction, such that simultaneous correction of distinct defects would achieve greater efficacy than correction of a single defect. One screen was done using cells expressing ΔF508-CFTR in which test compound was added together with VX-809, an established corrector that has been extensively characterized and is in clinical trials. Though the precise correction mechanism of VX-809 has not been resolved, current data suggests that VX-809 may target multiple sites at the NBD1-MSDs interface and interact with the N-terminal fragment of CFTR, represented by MSD1 or MSD1-NBD1 (Farinha et al., 2013; He et al., 2013; Loo et al., 2013; Okiyoneda et al., 2013; Ren et al., 2013). Mutagenesis studies and thermo-stabilization of ΔF508-CFTR suggest that VX-809 interacts directly with the channel (Okiyoneda et al., 2013), although indirect effects cannot be precluded. A second screen was done in cells expressing R1070W-ΔF508-CFTR (in the absence of VX-809), since in the background of genetically stabilized ΔF508-NBD1 the R1070W mutation was necessary and sufficient to restore robust CFTR domain assembly and cell surface expression (Mendoza et al., 2012; Rabeh et al., 2012; Thibadeau et al., 2010).

Screening was done using a human lung epithelium-derived cell line, CFBE41o-, that was stably transfected with HRP-tagged ΔF508-CFTR or R1070W-ΔF508-CFTR. The CFBE41o- cell line was selected as a readily transfectable cell line that is predicted to recapitulate the human bronchial epithelium (Ehrhardt et al., 2006). However, it is recognized that quality control mechanisms for ΔF508-CFTR processing are cell type-dependent (Pedemonte et al., 2010), so that there are potential concerns for screens done with any cell line. We note that VX-809 is an analog of a corrector identified in a ΔF508-CFTR mouse fibroblast cell line (Van Goor et al., 2010). The CFTR constructs used here for screening were engineered with an HRP in their fourth extracellular loop for robust plate reader-based luminescence measurements of cell surface CFTR expression. The constructs were transfected using a tetracycline-inducible promoter in order to prevent phenotypic drift of the CFBE41o- cells during

16

passages. The luminescence HRP assay significantly simplified the CFTR detection as compared to

HA-tagged variants (Okiyoneda et al., 2010), and increased signal-to-noise ratio, reproducibility and

dynamic range.

The screens identified small molecules that functioned as correctors when used individually, and,

when used together with VX-809, had greater efficacy than maximal VX-809 alone. Several classes of

compounds were identified that produced a greater than 140 % increase in HRP luminescence when

added with VX-809 in transfected CFBE41o- cells. These compounds were verified by independent

biochemical assays, either from accumulation of complex-glycosylated ΔF508-CFTR-3HA by

immunoblot (Supplemental Fig. 5) or cell surface ELISA in transfected CFBE41o- cells, thus

confirming the use of HRP-tagged CFTR as valid screening tool for modulators of ΔF508-CFTR

biogenesis. Most of the compounds were also active in a secondary functional assay done in

ΔF508-CFTR-transfected A549 cells, albeit with relative lower activity. The most active correctors in

A549 cells were class D and H correctors, having low micromolar potency. In primary human bronchial

cell cultures from a ΔF508 homozygous CF patient, most compounds, including the dihydrosprio-indene

H-01, showed little activity. Cell-specific corrector activity has been described (Pedemonte et al., 2010),

although the mechanisms responsible are not known. Of note, the 2-aminothiazole D-01 acted in

synergy with VX-809 in the ΔF508 human bronchial epithelia, increasing chloride current greater than

VX-809 alone. The substantial increase seen with forskolin alone in the D-01-treated cells suggests that

the D-01/VX-809 corrector combination is able to partially correct the ΔF508-CFTR folding defect.

Mechanistic studies suggested that D-01 is unable to stabilize the NBD1 thermodynamically, but likely

targets the NBD2 or its interface with NBD1 or MSDs, as the presence of the NBD2 is required for the

D-01 rescue effect and the domain deletion prevented the rescue of ΔF508-1218X-CFTR.

There are several prior reports on biological properties of the corrector scaffolds identified in this

study. We previously reported 2-aminoarylthiazole ΔF508-CFTR correctors that are structurally similar

to the 2-aminothiazoles (class D) identified here (Pedemonte et al., 2005a). Mechanism of action studies

suggested that 2-aminoarylthiazoles improved ΔF508-CFTR folding at the ER and stability at the cell

surface (Loo et al., 2008). Recent reported biological activities of aminothiazoles includes inhibition of

17

prion replication (Gallardo-Godoy et al., 2012), antimicrobial activity against methicillin-resistant *Staphylococcus aureus* (Annadurai et al., 2012), and γ-secretase modulators for treatment of Alzheimer's disease (Lübbers et al., 2011). Similar dihydrospiro-indenes (class H) have been reported as inhibitors of *Enterococeus faecalis* and *Staphylococcus aureus* phenylalanyl-*t*RNA synthetases with low nanomolar potency (Yu et al., 2004). Dihyrospiro-indenes have also been reported to be inhibitors of human papillomavirus type 11 (HPV11) E1-E2 protein-protein interaction (Goudreau et al., 2007). To our knowledge, the channel-modulating effects of dihydrospiro-indene have not been reported.

In summary, the results here provide proof-of-concept for the paradigm of synergy-based screening to identify corrector combinations with greater efficacy than individually used correctors, and support the idea that the ΔF508 mutation confers multiple structural defects in the CFTR chloride channel. While the compounds identified here produced only a modest increase in maximal correction efficacy, their activity and synergy with VX-809 in different human lung epithelial cell lines, including primary human bronchial cell cultures, supports further synergy screens to identify efficacious corrector combinations.

ACKONWLEDGMENTS

AUTHORSHIP CONTRIBUTIONS

Participated in research design: Phuan, Veit, Lukacs, and Verkman.

Conducted experiments: Phuan, Veit, Tan, and Roldan.

Wrote or contributed to the writing of the manuscript: Phuan, Veit, Roldan, Finkbeiner, Lukacs, and

Verkman.

REFERENCES

Accurso FJ, Rowe SM, Clancy JP, Boyle MP, Dunitz JM, Durie PR, Sagel SD, Hornick DB, Konstan MW, Donaldson SH, Moss RB, Pilewski JM, Rubenstein RC, Uluer AZ, Aitken ML, Freedman SD, Rose LM, Mayer-Hamblett N, Dong Q, Zha J, Stone AJ, Olson ER, Ordonez CL, Campbell PW, Ashlock MA, and Ramsey BW (2010) Effect of VX-770 in persons with cystic fibrosis and the G551D-CFTR mutation. *N Engl J Med* **363**: 1991-2003.

Annadurai S, Martinez R, Canney DJ, Eidem T, Dunman PM, and Abou-Gharbia M (2012) Design and synthesis of 2-aminothiazole based antimicrobials targeting MRSA. *Bioorg Med Chem Lett.* **22(24)**: 7719-7725.

Ashlock MA and Olson ER (2011) Therapeutics development for cystic fibrosis: a successful model for a multisystem genetic disease. *Annu Rev Med.* **62**: 107-125.

Balch WE, Roth DM, and Hutt DM (2011) Emergent properties of proteostasis in managing cystic fibrosis. *Cold Spring Harb Perspect Biol.* **3(2)**: a004499.

Blanchard E, Zlock L, Lao A, Mika D, Namkung W, Xie M, Scheitrum C, Gruenert DC, Verkman AS, Finkbeiner WE, Conti M, and Richter W. (2014) Anchored PDE4 regulates chloride conductance in wild-type and ΔF508-CFTR human airway epithelia. *FASEB J.* **28(2):**791-801.

Boucher RC (2004) New concepts of the pathogenesis of cystic fibrosis lung disease. *Eur Respir J.* **3(1)**: 146-158.

Clancy JP, Rowe SM, Accurso FJ, Aitken ML, Amin RS, Ashlock MA, Ballmann M, Boyle MP, Bronsveld I, Campbell PW, De Boeck K, Donaldson SH, Dorkin HL, Dunitz JM, Durie PR, Jain M, Leonard A, McCoy KS, Moss RB, Pilewski JM, Rosenbluth DB, Rubenstein RC, Schechter MS, Botfield M, Ordoñez CL, Spencer-Green GT, Vernillet L, Wisseh S, Yen K, and Konstan MW (2012) Results of a phase IIa study of VX-809, an investigational CFTR corrector compound, in subjects with cystic fibrosis homozygous for the F508del-CFTR mutation. *Thorax.* **67(1)**: 12-18.

Cohen TS and Prince A (2012) Cystic fibrosis: a mucosal immunodeficiency syndrome. *Nat Med.* **18(4)**: 509-519.

Du K and Lukacs GL (2009) Cooperative assembly and misfolding of CFTR domains in vivo. *Mol Biol*

Cell. **20(7)**: 1903-1915.

Ehrhardt C, Collnot EM, Baldes C, Becker U, Laue M, Kim KJ, and Lehr CM (2006) Towards an in vitro model of cystic fibrosis small airway epithelium: characterisation of the human bronchial epithelial cell line CFBE41o-. *Cell Tissue Res.* **323(3)**: 405-415.

Farinha CM, King-Underwood J, Sousa M, Correia AR, Henriques BJ, Roxo-Rosa M, Da Paula AC, Williams J, Hirst S, Gomes CM, and Amaral MD (2013) Revertants, low temperature, and correctors reveal the mechanism of F508del-CFTR rescue by VX-809 and suggest multiple agents for full correction. *Chem Biol.* **20(7)**: 943-955.

Fulcher ML and Randell SH (2013) Human nasal and tracheo-bronchial respiratory epithelial cell culture. *Methods Mol Biol.* **945**: 109-121.

Gadsby DC, Vergani P, and Csanády L (2006) The ABC protein turned chloride channel whose failure causes cystic fibrosis. *Nature* **440(7083)**: 477-483.

Galietta LJ, Haggie PM, and Verkman AS (2001) Green fluorescent protein-based halide indicators with improved chloride and iodide affinities. *FEBS Lett*. **499**: 220-224.

Gallardo-Godoy A, Gever J, Fife KL, Silber BM, Prusiner SB, and Renslo AR (2011) 2-Aminothiazoles as therapeutic leads for prion diseases. *J Med Chem.* **54(4)**:1010-1021.

Goudreau N, Cameron DR, Déziel R, Haché B, Jakalian A, Malenfant E, Naud J, Ogilvie WW, O'Meara J, White PW, and Yoakim C (2007) Optimization and determination of the absolute configuration of a series of potent inhibitors of human papillomavirus type-11 E1-E2 protein-protein interaction: a combined medicinal chemistry, NMR and computational chemistry approach. *Bioorg Med Chem.* **15(7)**, 2690-2700.

Hanrahan JW, Sampson HM, and Thomas DY (2013) Novel pharmacolostrategies to treat cystic fibrosis. *Trends Pharmacol Sci.* **34(2)**, 119-125.

He L, Kota P, Aleksandrov AA, Cui L, Jensen T, Dokholyan NV, and Riordan JR (2013) Correctors of ΔF508 CFTR restore global conformational maturation without thermally stabilizing the mutant protein. *FASEB J.* **27(2)**, 536-545.

Loo TW, Bartlett MC, and Clarke DM (2013) Corrector VX-809 stabilizes the first transmembrane

domain of CFTR. *Biochem Pharmacol.* **86(5)**, 612-619.

Lübbers T, Flohr A, Jolidon S, David-Pierson P, Jacobsen H, Ozmen L, and Baumann K. (2011) Aminothiazoles as γ-secretase modulators. *Bioorg Med Chem Lett.* **21(21)**: 6554-6558.

Lukacs GL and Verkman AS (2012) CFTR: folding, misfolding and correcting the ΔF508 conformational defect. *Trends Mol Med.* **18(2)**: 81-91.

Mendoza JL, Schmidt A, Li Q, Nuvaga E, Barrett T, Bridges RJ, Feranchak AP, Brautigam CA, and Thomas PJ (2012) Requirements for efficient correction of ΔF508 CFTR revealed by analyses of evolved sequences. *Cell* **148(1-2)**: 164-174.

Okiyoneda T, Barriere H, Bagdany M, Rabeh WM, Du K, Hohfeld J, Young JC, and Lukacs GL (2010) Peripheral protein quality control removes unfolded CFTR from the plasma membrane. *Science* **329**: 805-810.

Okiyoneda T, Veit G, Dekkers JF, Bagdany M, Soya N, Xu H, Roldan A, Verkman AS, Kurth M, Simon A, Hegedus T, Beekman JM, and Lukacs GL (2013) Mechanism-based corrector combination restores ΔF508-CFTR folding and function. *Nat Chem Biol.* **9(7)**: 444-454.

Okiyoneda T and Lukacs GL (2012) Fixing cystic fibrosis by correcting CFTR domain assembly. *J Cell Biol.* **199(2)**: 199-204.

Pedemonte N, Lukacs GL, Du K, Caci E, Zegarra-Moran O, Galietta LJ, and Verkman AS (2005a) Small-molecule correctors of defective ΔF508-CFTR cellular processing identified by high-throughput screening. *J Clin Invest.* **115**: 2564-2571.

Pedemonte N, Sonawane ND, Taddei A, Hu J, Zegarra-Moran O, Suen YF, Robins LI, Dicus CW, Willenbring D, Nantz MH, Kurth MJ, Galietta LJ, and Verkman AS (2005b) Phenylglycine and sulfonamide correctors of defective ΔF508 and G551D cystic fibrosis transmembrane conductance regulator chloride-channel gating. *Mol Pharmacol.* **67**: 1797-1807.

Pedemonte N, Tomati V, Sondo E, and Galietta, LJ (2010) Influence of cell background on pharmacological rescue of mutant CFTR. *Am J Physiol Cell Physiol.* **298**: C866-874.

Phuan PW, Yang B, Knapp JM, Wood, AB, Lukacs GL, Kurth MJ, and Verkman AS (2011) Cyanoquinolines with independent corrector and potentiator activities restore ΔF508-CFTR

chloride channel function in cystic fibrosis. *Mol. Pharmacol.* **80**: 683-693.

Rabeh WM, Bossard F, Xu H, Okiyoneda T, Bagdany M, Mulvihill CM, Du K, di Bernardo S, Liu Y, Konermann L, Roldan A, and Lukacs GL (2012) Correction of both NBD1 energetics and domain interface is required to restore ΔF508 CFTR folding and function. *Cell* **148(1-2)**: 150-163.

Ren HY, Grove DE, De La Rosa O, Houck SA, Sopha P, Van Goor F, Hoffman BJ, and Cyr DM (2013) VX-809 corrects folding defects in CFTR through action on membrane-spanning domain1 (MSD1). *Mol Biol Cell.* **24(19)**: 3016-3024.

Riordan JR (2005) Assembly of functional CFTR chloride channels. *Annu Rev Physiol.* **77**: 701-726.

Riordan JR (2008) CFTR function and prospects for therapy. *Annu Rev Biochem.* **77**: 701-726.

Robert R, Carlile GW, Liao J, Balghi H, Lesimple P, Liu N, Kus B, Rotin D, Wilke M, de Jonge HR, Scholte BJ, Thomas DY, and Hanrahan JW (2010) Correction of the Delta phe508 cystic fibrosis transmembrane conductance regulator trafficking defect by the bioavailable compound glafenine. *Mol Pharmacol* **77**: 922-930.

Sato S, Ward CL, Krouse ME, Wine JJ, and Kopito RR (1996) Glycerol reverses the misfolding phenotype of the most common cystic fibrosis mutation. *J Biol Chem.* **271**: 635-638.

Thibodeau PH, Richardson JM 3rd, Wang W, Millen L, Watson J, Mendoza JL, Du K, Fischman S, Senderowitz H, Lukacs GL, Kirk K, and Thomas PJ (2010) The cystic fibrosis-causing mutation ΔF508 affects multiple steps in cystic fibrosis transmembrane conductance regulator biogenesis. *J Biol Chem.* **285**: 35825-35835.

Van Goor F, Hadida S, Grootenhuis PD, Burton B, Cao D, Neuberger T, Turnbull A, Singh A, Joubran J, Hazlewood A, Zhou J, McCartney J, Arumugam V, Decker C, Yang J, Young C, Olson ER, Wine JJ, Frizzell RA, Ashlock M, and Negulescu P (2009) Rescue of CF airway epithelial cell function in vitro by a CFTR potentiator, VX-770. *Proc Natl Acad Sci U S A.* **106(44)**: 18825-18830.

Van Goor F, Hadida, S., Grootenhuis, PD., Burton, B., Stack, JH., Straley, KS., Decker, CJ., Miller, M., McCartney, J., Olson, ER., Wine, JJ., Frizzell, RA., Ashlock, M., and Negulescu, PA (2011) Correction of the F508del-CFTR protein processing defect in vitro by the investigational drug VX-809. *Proc Natl Acad Sci U S A.* **108(46)**: 18843-18848.

Van Goor F, Straley KS, Cao D, Gonzalez J, Hadida S, Hazlewood A, Joubran J, Knapp T, Makings LR, Miller M, Neuberger T, Olson E, Panchenko V, Rader J, Singh A, Stack JH, Tung R, Grootenhuis PD, and Negulescu P (2006) Rescue of ΔF508-CFTR trafficking and gating in human cystic fibrosis airway primary cultures by small molecules. *Am J Physiol Lung Cell Mol Physiol*. **290**: L1117-1130.

Veit G, Bossard F, Goepp J, Verkman AS, Galietta LJ, Hanrahan JW, and Lukacs GL (2012) Proinflammatory cytokine secretion is suppressed by TMEM16A or CFTR channel activity in human cystic fibrosis bronchial epithelia. *Mol Biol Cell.* **23(21):** 4188-4202.

Yamaya M, Finkbeiner WE, Chun SY, and Widdicombe JH (1992) Differentiated structure and function of cultures from human tracheal epithelium. *Am J Physiol 262 (Lung Cell Mol Physiol 6)***:** L713-L724.

Yu XY, Finn J, Hill JM, Wang ZG, Keith D, Silverman J, and Oliver N (2004) A series of spirocyclic analogues as potent inhibitors of bacterial phenylalanyl-tRNA synthetases. *Bioorg Med Chem Lett.* **14(5)**: 1339-1342.

Yu GJ, Yoo CL, Yang B, Lodewyk MW, Meng L, El-Idreesy TT, Fettinger JC, Tantillo DJ, Verkman AS, and Kurth MJ (2008) Potent s-cis-locked bithiazole correctors of ΔF508 cystic fibrosis transmembrane conductance regulator cellular processing for cystic fibrosis therapy. *J Med Chem.* **51**: 6044-6054.

Zielenski J (2000) Genotype and phenotype in cystic fibrosis. *Respiration.* **67(2)**: 117-33.

Zhang JH, Chung TD, Oldenburg KR (1999) A Simple Statistical Parameter for Use in Evaluation and Validation of High Throughput Screening Assays. *J Biomol Screen* **4(2)**: 67-73.

MOL #92478

FIGURE LEGENDS

Figure 1. **High-throughput synergy screens for identification of ΔF508-CFTR correctors.**

A. Screening assay for ΔF508-CFTR-HRP CFBE41o cells (top) showing incubation with 25 μM test compounds and 2 μM VX-809 for 24 h at 37 ℃. Cell surface ΔF508-CFTR was assayed by a luminescence readout of HRP activity. Concentration-dependence data (bottom left) and bar graph for luminescence readout of VX-809 effect (S.E., n = 4) at 27 and 37 ℃. **B.** Screening assay for R1070W-ΔF508-CFTR-HRP CFBE41o cells (top) showing incubation with 25 μM test compounds for 24 h at 37 ℃. Concentration-dependence data (bottom left) and bar graph for luminescence readout of VX-809 effect (S.E., n = 4) at 27 and 37 ℃.

Figure 2. **Screening results. A**. Summary of primary findings of the ΔF508-CFTR screen. **B.** Chemical structures of three classes of correctors identified from the screen. **C**. Summary of primary findings of the R1070W-ΔF508-CFTR screen. **D.** Chemical structures of six classes of correctors identified from the screen.

Figure 3. **Corrector concentration-dependence studies. A.** Concentration-dependence data of A-01, B-01, H-01 and K-01, with 2 μM VX-809, in ΔF508-CFTR-HRP CFBE41o- cells (S.E., n = 3). **B.** Concentration- dependence data of A-01, B-01, D-01, H-01 and K-01 in R1070W-ΔF508-CFTR-HRP CFBE41o- cells (S.E., n = 3). **C.** Correlation between PM density of ΔF508-HRP and ΔF508-3HA in CFBE41o- cells treated with correctors (5 and 25 μM, 24 h, 37 ℃) alone or in combination with 3 μM VX-809. Data were fitted by linear regression analysis with $R^2 = 0.94$ (S.E., $n = 3$).

Figure 4. **Structure-activity relationships of class D and H compounds. A.** Concentration-dependence data of class D analogs in R1070W-ΔF508-CFTR-HRP CFBE41o- cells (S.E., n = 3). **B.** Structural determinants of corrector activity of class D compounds. **C.** Concentration-dependence data of class H analogs, together with 2 μM VX-809, in ΔF508-CFTR-HRP CFBE41o- cells (S.E., n = 3). **D.** Structural determinants of corrector activity of class H compounds. Control-(DMSO) background corrected

luminescence signals.

Figure 5. **Functional assay in A549 cells expressing ΔF508-CFTR and a halide-sensitive YFP.**

A. Assay schematic. A549 cells were incubated with test compounds, with or without 2 μM VX-809, at 37 °C for 24 h. ΔF508-CFTR function was assayed in a plate reader from the kinetics of YFP fluorescence quenching in response to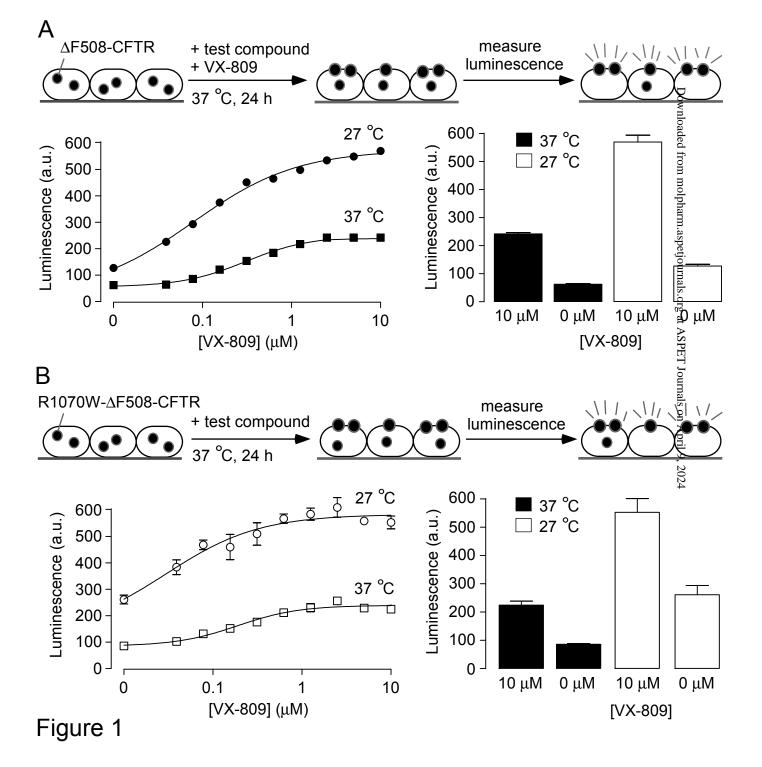 extracellular iodide addition in the presence of forskolin (20 μM) and genistein (50 μM). **B.** Representative data curves showing iodide influx at different [D-01] and [H-01], without and with 2 μM VX-809. **C.** Concentration-dependence data of A-01, B-01, D-01, H-01 and K-01, without and with 2 μM VX-809 (S.E., n = 3). Fitted curves for single-site activation model.

Figure 6. **Corrector mechanism of action. A.** Plasma membrane expression of temperature-rescued (26 °C, 48 h) HRP-CD4TM-ΔF508-NBD1-1S in MDCK cells. Cells were treated with the indicated correctors for 24 h at 26 °C followed by 1 h chase at 37 °C. **B.** Representative melting curves (left panel) and melting temperature (Tm, right panel) of human ΔF508-NBD1-1S determined by differential scanning fluorimetry. C-01, D-01 or H-01, or the chemical chaperone glycerol, were present during thermal unfolding at the indicated concentrations. **C.** Relative effect of corrector 4 (10 μM, 24 h, 37 °C) on the PM density of R1070W-HRP CFBE41o- cells treated with A-01 – D-01, H-01, J-01, K-01 or VX-809 at the indicated concentrations. **D.** PM density of ΔF508-CFTR-3HA and ΔF508-1218X-CFTR-3HA treated with D-01 (5 and 25 μM, 24 h, 37 °C) alone (left panel) or in combination with VX-809 (right panel) in BHK cells. Errors represent means ± SEM of three independent experiments (B, D) or means ± SD of 8 measurements in two independent experiments (A, C). *, $p < 0.05$; **, $p < 0.01$ by unpaired t-test.

Figure 7. **Functional assays in primary cultures of human bronchial epithelial cells from a homozygous ΔF508 CF patient. A.** Representative short-circuit current recordings. Cells were incubated at 37 °C for 24 h with DMSO vehicle, 10 μM VX-809, 30 μM D-01 or 10 μM VX-809 + 30 μM D-01. Concentrations were: amiloride, 10 μM; forskolin, 20 μM; genistein, 50 μM; $CFTR_{inh}$-172, 10

μM. **B**. Summary of changes in short-circuit current (ΔI_{sc}) produced by forskolin alone and forskolin + genistein from experiments as in A (S.E.; $n = 3$ cultures each). *, $p < 0.05$; by unpaired t-test.

Figure 1

A
ΔF508-CFTR
primary screen
50,000 compounds
↓
164 hits (>50 % luminescence
signal over 2 µM VX-809)
↓
5 confirmed hits
↓
3 compound classes (H, J, K)

B

H-01

J-01

K-01

C
R1070W-ΔF508-CFTR
primary screen
60,240 compounds
↓
25 hits (>50% luminescence
signal over DMSO control)
↓
9 confirmed hits
↓
6 compound classes (A, B, C, D, E, F)

D

A-01

B-01

C-01

D-01

E-01

F-01

Figure 2

A ΔF508-CFTR

B R1070W-ΔF508-CFTR

C

Figure 3

A

R1070W-ΔF508-CFTR

B Class D - aminothiazoles

active ring =

inactive ring =

best R^1 =

inactive R^1 =

C

ΔF508-CFTR

D Class H - dihydrospiro-indene

best R^1 = 4-substituted halides, methyl, ethyl, isopropyl

inactive R^2 = 2-substitution, 4-CO_2Et

best R^2 =

inactive R^2 =

n = 1,2

Figure 4

A

ΔF508-CFTR

test compound
± VX-809

20 μM fsk.
50 μM gen.
37 °C, 24 h

+ I⁻

I⁻   I⁻   I⁻
I⁻   I⁻
I⁻

B

[D-01] (μM) =

normalized fluor.

1.0

0   1.5   3   6   12   25

0.8

5 s

0.6

+ 2 μM VX-809

[D-01] (μM) =

0   1.5   3   6   12   25

[H-01] (μM) =

0   1.5   3   6   12

+ 2 μM VX-809

[H-01] (μM) =

0   1.5   3   6   12

C

slope

40   2 μM VX-809

30   B-01   A-01
            D-01
20
                         K-01   H-01
10
      0 μM VX-809

0
0.1   1   10   30
[corrector] (μM)

50   H-01   B-01
          D-01
40
                      A-01   K-01
                   2 μM VX-809
30

0
0.1   1   10   30
[corrector] (μM)

Figure   5

Figure 6

A ΔF508/ΔF508 human bronchial cells

amiloride, CFTR$_{inh}$-172, fsk, gen, CFTR$_{inh}$-172

3 μA/cm^2

5 min

+ VX-809 (10 μM)

amiloride, fsk, gen, CFTR$_{inh}$-172

+ D-01 (30 μM)

amiloride, fsk, gen, CFTR$_{inh}$-172

+ VX-809 (10 μM)
+ D-01 (30 μM)

B

control, VX-809, D-01, VX-809 + D-01

*

ΔI$_{sc}$ (μA/cm^2)

forskolin

control, VX-809, D-01, VX-809 + D-01

*

ΔI$_{sc}$ (μA/cm^2)

forskolin + genistein

Figure 7